Proceedings of the
Annual Stability Conference
Structural Stability Research Council
San Antonio, Texas, March 21-24, 2017

Stability analysis of steel columns under cascading-hazard of earthquake and fire

Mehrdad Memari[1], Hussam Mahmoud[2]

Abstract

Stability analysis of steel structures under elevated temperatures remains a challenging design problem because of the uncertainties associated with fire loads, temperature-dependent material properties, non-uniform heating of structural members, and large deformational demands on the steel frames. The challenge is further aggravated if the stability of the system is also influenced by the permanent lateral deformation due to the earthquake preceding the thermal loads. The present study discusses a framework for assessing the stability of steel columns under inter-story drift imposed by the earthquake followed by fire loads. A nonlinear finite element formulation is proposed to analyze the stability of steel columns subjected to permanent lateral deformations caused by earthquake and fire loads. The finite element formulation takes into account the effects of longitudinal temperature variation in first- and second-order stiffness matrices of a beam-column element, residual stresses, and initial geometric imperfections. The results indicate an excellent agreement with available strength design equations of steel columns at ambient and elevated temperatures. A set of equations is then proposed to predict the critical buckling stress in steel columns under fire and fire following an earthquake. The proposed equations can be implemented to investigate the performance of steel structures under fire and fire following earthquake considering stability as engineering demand parameter.

1. Introduction

Strong earthquakes can cause fatalities and severe damages to civil infrastructures by shaking, landslide, liquefaction, tsunami, fire, and release of hazardous materials. In the steel framed buildings, the earthquake-induced damages to gravity and lateral load resisting systems can significantly reduce post-earthquake fire resistance of the structure. This is particularly the case because current seismic design codes allow buildings to sustain a certain level of damages caused by strong earthquakes. Therefore, properly designed buildings for seismic actions can be significantly vulnerable under post-earthquake fire loads. Because columns are the most important members in resisting gravity loads in a building system, their stability under fire has been the focus of several previous studies (Franssen et al. 1998, Takagi and Deierlein 2007, Agarwal and Varma 2011). The stability of steel moment resisting frames under fire (Memari

[1] Postdoctoral Fellow, Colorado State University, <mehrdad.memari@colostate.edu>
[2] Assistant Professor, Colorado State University, <hussam.mahmoud@colostate.edu>

and Mahmoud 2014) and the combined loads of earthquake and fire (Memari et al. 2014) has also been evaluated in recent studies. These studies highlighted the importance of improving understanding of the behavior of steel columns subjected to non-uniform longitudinal temperature and inter-story drift ratio (IDR).

Takagi and Deierlein (2007) evaluated the AISC Specification (AISC 360-05 2005) and Eurocode 3 (CEN 2005) provisions for the design of isolated W-shape steel columns under elevated temperatures that were uniform along the length of the column. The numerical model of columns was developed using shell elements to account for local buckling. The outcome of this study was the design equation for W-shape steel columns under a uniform longitudinal temperature that currently appears in Appendix 4, Equation A-4-2, of AISC Specification (AISC 360-10 2010).

Another important study to note is the work by Agarwal and Varma (2011) who utilized comprehensive finite element analyses to assess the effects of slenderness and rotational restraints on the buckling response of W-shaped steel columns subjected to uniform elevated temperatures. Shell elements were also used to create the numerical models because of their ability in capturing local buckling and inelastic flexural-torsional buckling. The study resulted in the new design equations for simply supported columns with uniform longitudinal temperature distribution considering an equivalent bilinear material behavior. The effects of rotational constraints, provided by continuity with cooler columns above and below the column of interest in a structural frame, were also included in the proposed design equations.

Extending the work by Takagi and Deierlein (2007) and Agarwal and Varma (2011), in this paper, a nonlinear finite element formulation is introduced to perform the stability analysis of W-shape steel columns subjected to non-uniform longitudinal temperature profiles in the absence or presence of inter-story drift, which represent residual drift following an earthquake. This formulation takes into account the residual stress distribution in steel hot-rolled W-shape sections, initial geometric imperfections in the steel columns, and temperature-dependent material properties. The results of the finite element analysis (FEA) are verified against comparison with previous studies. Afterward, a set of equations is proposed for predicting the critical buckling stress in steel columns subjected to the cascading hazard of earthquake, represented by lateral drift, and fire, represented with non-uniform longitudinal temperature distributions.

2. Modeling and Analysis Methodology

2.1 Finite Element Formulation

A finite element formulation is utilized to predict the onset of instability of steel columns subjected to an inter-story drift level followed by non-uniform longitudinal temperature distribution. Euler-Bernoulli beam theory is employed assuming a constant temperature profile throughout the cross section of the element. This finite element formulation is created based on studies conducted by Carol and Murcia (1989) and Memari and Attarnejad (2010). In addition, the details of the formulation have been discussed in Memari et al. (2016) and Memari (2016). In this formulation, a finite element is assumed to have a non-uniform longitudinal temperature distribution with T_i and T_j as the nodal temperatures at either end as shown in Fig. 1.

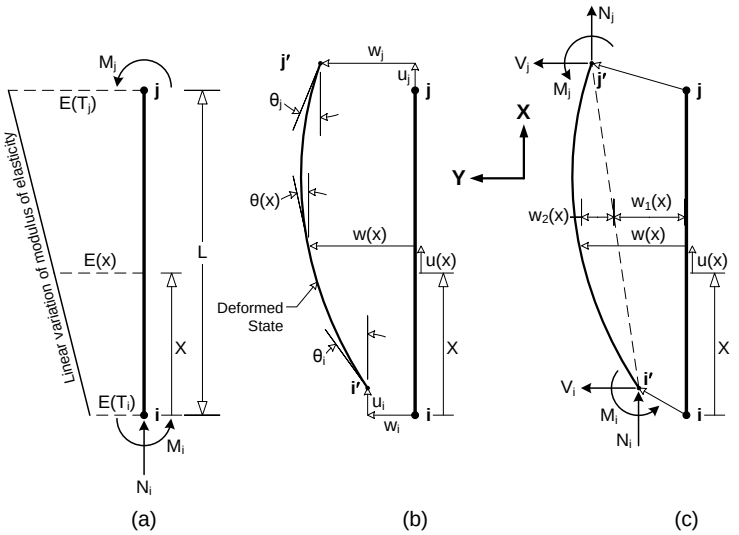

Figure 1: (a) A finite element with linear variation of modulus of elasticity along its length and three applied external nodal forces, (b) the deformed state of the finite element with all nodal deformation variables, and (c) the deformed state of the finite element with all nodal force variables

Since the modulus of elasticity of structural steel is a function of temperature, a linear variation of temperature-dependent modulus of elasticity, E(x), is assumed along the length of the finite element per Eq. 1, in which ζ is calculated according to Eq. 2. To model the entire column, a sufficient number of finite elements can be utilized such that the linear variation of elastic modulus along each element results in capturing of the nonlinear variation along the entire length of the column.

$$E(x) = E(T_i)\left(1 + \frac{\zeta x}{L}\right) \tag{1}$$

$$\zeta = \frac{E(T_j)}{E(T_i)} - 1 \tag{2}$$

In this approach, three sets of equations are considered in developing first- and second-order stiffness matrices: kinematic equation (Eq. 3), 2nd-order equilibrium (Eq. 4), and constitutive law (Eq. 5). In accordance with the deformed state of the finite element shown in Fig. 1(b), the kinematic equation relates the relative displacements and rotations to the field of axial strain at the neutral axis of the section, ε, and curvature, φ. The cross-sectional axial force, N(X), and bending moment, M(x), is determined based on applied nodal axial force, Ni, and nodal moments, M_i and M_j, using equilibrium equations per Eq. 4 including the second-order (P- δ) effects, shown in Fig. 1(c). The cross-sectional strain and curvature can be also related to the cross-sectional forces and moments per Eq. 5 under the assumption that the element responds elastically to the nodal forces. It is noted that the compact form of Eq.'s 3-5 is shown in the brackets. In Eq. 3, *u* demonstrates a vector of relative displacements and rotations, Ω is a transformation matrix that converts strains to displacements and rotations, and γ is called vector of strains. In Eq. 5, $w_2(x)$ is the out-of-straightness curvature of the finite element that causes the P-δ effects. R(x) is a vector of internal cross-sectional forces developed at the inclusion of 2nd-

order effects, $R_2(x)$. The vector *f* represents the applied nodal forces and moments and Ω is a matrix that correlates the applied nodal forces to those developed internally in the cross-section. In Eq. 6, A and I are cross-sectional area and moment of inertia, respectively. $\mathbf{k_s(x)}$ is called cross-sectional stiffness matrix. The remainder of variables was shown in Fig. 1.

$$\begin{bmatrix} -(u_j - u_i) \\ \frac{w_j - w_i}{L} - \theta_i \\ \theta_j - \frac{w_j - w_i}{L} \end{bmatrix} = \int_0^L \begin{bmatrix} 1 & 0 \\ 0 & 1 - \frac{x}{L} \\ 0 & \frac{x}{L} \end{bmatrix} \begin{bmatrix} \varepsilon \\ \varphi \end{bmatrix} dx \qquad (3)$$

$$\{ u = \int_0^L \Omega^T . \gamma dx \}$$

$$\begin{bmatrix} N(x) \\ M(x) \end{bmatrix} = \begin{bmatrix} 1 & 0 & 0 \\ 0 & 1 - \frac{x}{L} & \frac{x}{L} \end{bmatrix} \begin{bmatrix} N_i \\ M_i \\ M_j \end{bmatrix} + \begin{bmatrix} 0 \\ -N_i . w_2(x) \end{bmatrix} \qquad (4)$$

$$\{ \mathbf{R(x)} = \Omega . \mathbf{f} + \mathbf{R_2(x)} \}$$

$$\begin{bmatrix} N(x) \\ M(x) \end{bmatrix} = \begin{bmatrix} E(x)A & 0 \\ 0 & E(x)I \end{bmatrix} \begin{bmatrix} \varepsilon \\ \varphi \end{bmatrix} \qquad (5)$$

$$\{ R(x) = \mathbf{k_s(x)} . \gamma \}$$

The longitudinal variation in the modulus of elasticity, caused by the non-uniform temperature distribution, is reflected in the cross-sectional stiffness matrix by substituting the Eq. 1 into Eq. 5 as follows:

$$\mathbf{k_s(x)} = E(T_i)\left(1 + \frac{\zeta x}{L}\right) \begin{bmatrix} A & 0 \\ 0 & I \end{bmatrix} \qquad (6)$$

Eq. 6 clearly indicates that the section stiffness varies along the length of element as a function of the elastic modulus. This important feature allows for considering the effects of non-uniform longitudinal temperature distribution in developing first- and second-order stiffness matrices. These stiffness matrices, necessary for the stability analysis, can be extracted from above-discussed three sets of kinematic, equilibrium, and material law equations by substituting the equilibrium equation (Eq. 4) and constitutive law (Eq. 5) into the kinematic equation (Eq. 3). Further details are provided in Memari et al. (2016) and Memari (2016). In summary, the first- and second-order stiffness matrices of a beam-column finite element are developed to reflect non-uniform temperature variation along the length of the finite elements while a uniform temperature distribution is assumed through the cross section. The sources of initial geometric imperfections including out-of-straightness and out-of-plumbness are independently considered in the geometry of the columns for the nonlinear inelastic analysis. The out-of-straightness is modeled by introducing a single sinusoidal curve along the length of the column such that a

maximum displacement of 0.001 of column length is located at its mid-height. In addition, an initial out-of-plumbness of 0.001 of length of column is assumed at the top end of the column and the lateral nodal displacement for the remaining nodes is calculated accordingly.

2.2 Temperature-Dependent Mechanical Properties of Material

An elastic-perfectly plastic behavior of structural steel is assumed at ambient temperature, 68°F (20°C), as shown in Fig. 2(a). At elevated temperatures, a curvilinear material behavior per Fig. 2(a) is utilized as it has a significant effect on the critical buckling stress of steel columns (Takagi and Deierlein 2007, Agarwal and Varma 2011). Therefore, three mechanical properties of structural steel are considered in the stability analysis of steel columns exposed to elevated temperatures: modulus of elasticity (E), proportional limit (F_p), and yield stress (F_y). Temperature-dependent mechanical properties of structural steel are modeled per Eurocode 3 (CEN 2005), as shown in Fig. 2(a). The variations in E, F_p, and F_y as a function of temperature, described by β_E, β_p, and β_y, respectively, for Eurocode 3 (CEN 2005) stress-strain curves are shown in Fig. 2(b). It is noted that the temperature-dependent material properties according to Eurocode 3 (CEN 2005) inherently captures creep effects.

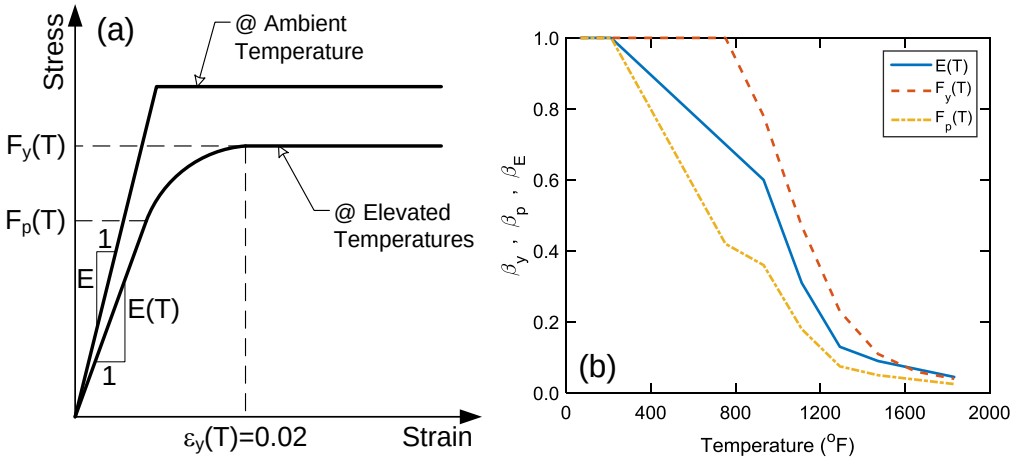

Figure 2: A schematic explanation of material modeling (a) Eurocode 3 (CEN 2005) and (b) variations in modulus of elasticity, yield stress, and proportional limit in accordance with Eurocode 3 (CEN 2005)

2.3 Non-uniform Longitudinal Temperature Profiles

A uniform temperature is assumed across the W-shape steel section in accordance with the AISC 360-10 (2010) design recommendations. The uniform longitudinal temperature profiles will be mainly used for validation analyses; however, non-uniform longitudinal temperature distributions are employed to investigate the critical buckling stress of steel columns under either single-hazard of fire or multiple-hazard of the earthquake and fire. In the present study, four various non-uniform longitudinal temperature profiles are considered in the steel columns as shown in Table 1, which summarizes longitudinal reduction of temperature-dependent mechanical properties from the cool-end to hot-end of the steel column. The temperature intervals were selected such that they capture various rates of longitudinal change in temperature-dependent mechanical properties of structural steel.

Table 1: Longitudinal variation of mechanical properties of structural steel according to non-uniform temperature profiles

Profile	Temperature at cool-end °F (°C)	Temperature at hot-end °F (°C)	Longitudinal relative reduction of mechanical properties between cool- and hot-end of steel column (%)		
			Modulus of elasticity	Yield stress	Proportional limit
(1)	68 (20)	572 (300)	20.0	0.0	38.7
(2)	392 (200)	932 (500)	33.3	22.0	55.4
(3)	572 (300)	1112 (600)	61.3	53.0	70.6
(4)	752 (400)	1472 (800)	87.1	89.0	88.1

The pattern of longitudinal temperature distribution is also an important parameter to be considered. In this paper, two longitudinal temperature distributions are considered: Parabolic and Linear. It is essential to evaluate the critical buckling stress of steel columns with parabolic distribution of temperature along the length because the solution of the governing 1-D Partial Differential Equation (PDE) for conduction heat transfer shows a parabolic function along the length of steel member at time t. However, since the requirements in code provisions to determine the parabolic distribution of temperature along the length of the member impose difficulties in real world engineering applications, a linear longitudinal distribution of temperature is also considered. This is to assess the difference in the results when using the two different longitudinal temperature patterns and evaluate the effectiveness of linear distribution on the results that might be considered acceptable.

2.4 Nonlinear Inelastic Analysis

A W14×90 section, made from A992 structural steel, is selected for the nonlinear inelastic analysis. To determine the critical buckling stress in a simply supported column, the applied compressive force at the top of the column is increased incrementally until the onset of buckling in the column. Per AISC Specification (AISC 360-10 2010), columns with slenderness ratio, λ, less than $4.71\sqrt{E/F_y}$ at ambient temperature are vulnerable to inelastic buckling, while columns with slenderness greater than $4.71\sqrt{E/F_y}$ buckle elastically. Therefore, it is crucial that this distinction be captured in the nonlinear finite element analysis. This is performed by defining two independent buckling limit states. The onset of compressive yielding at any cross section of steel column, based on the temperature-dependent yield stress, is chosen as the limit state for the inelastic buckling. The effects of temperature-dependent residual stresses are taken into account in the calculation of stress as shown in Fig. 3. A maximum of 10 ksi (~70 MPa) thermally-induced residual stresses is assumed at ambient temperature. The reduction factor for yield stress at elevated temperatures is also employed to reduce the intensity of the residual stresses in the cross section. This assumption was made by Takagi and Deierlein (2007). To determine the elastic buckling, the lateral stiffness of the column at a given loading increment is compared to the initial lateral stiffness of the column, which is calculated based on first increment of loading. Initial investigation of the developed formulation shows that the onset of elastic buckling is reached when the column loses 96% or more of its initial lateral stiffness.

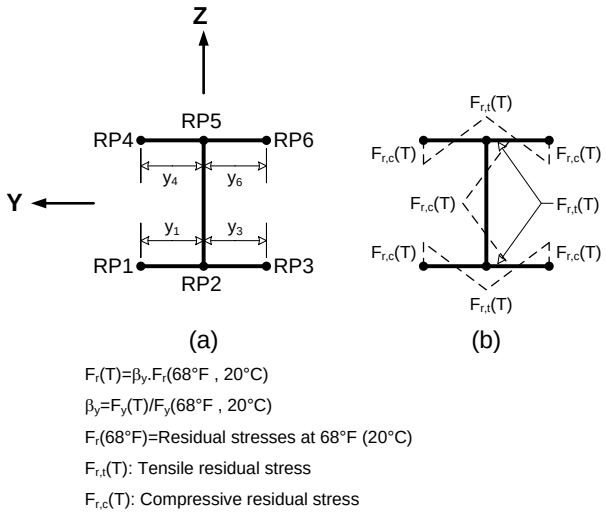

Figure 3: (a) 6 reference points and (b) distribution of residual stresses in W-shape steel section

2.5 Verification of the Formulation

A set of analyses is performed to verify the finite element formulation in the present study. This includes evaluating buckling of a pinned-pinned column at ambient and uniform longitudinal elevated temperatures using the W14×90 steel section considered previously. Details of the column are shown in Fig. 4(a). The material model utilized is shown in Fig. 2 for ambient and elevated temperatures. In addition, the effect of out-of-plumbness is neglected in the verification analysis since it is not reflected in the AISC Specification (AISC 360-10 2010) for critical buckling stress of members under compressive forces. However, initial out-of-straightness is considered per AISC Specification (AISC 360-10 2010).

At ambient temperature, the results of the finite element analysis are compared to the column buckling stress, F_{cr}, calculated using equations E3 and E4 of the AISC Specification (AISC 360-10 2010). As shown in Fig. 4(b), excellent agreement is observed between the critical buckling stresses determined by the finite element analysis and that of the AISC Specification (AISC 360-10 2010) design equation. Verification of the column stability at elevated temperatures is conducted by comparing the results of the finite element formulation to those of the column buckling equation proposed by Takagi and Deierlein (2007), available in Appendix 4 of AISC specifications (AISC 360-10 2010). The comparison is performed at two temperatures: 752°F (400°C) and 1472°F (800°C). Excellent agreements are also observed between the results of finite element formulation and the equations available in Appendix 4 of the AISC Specification (AISC 360-10 2010).

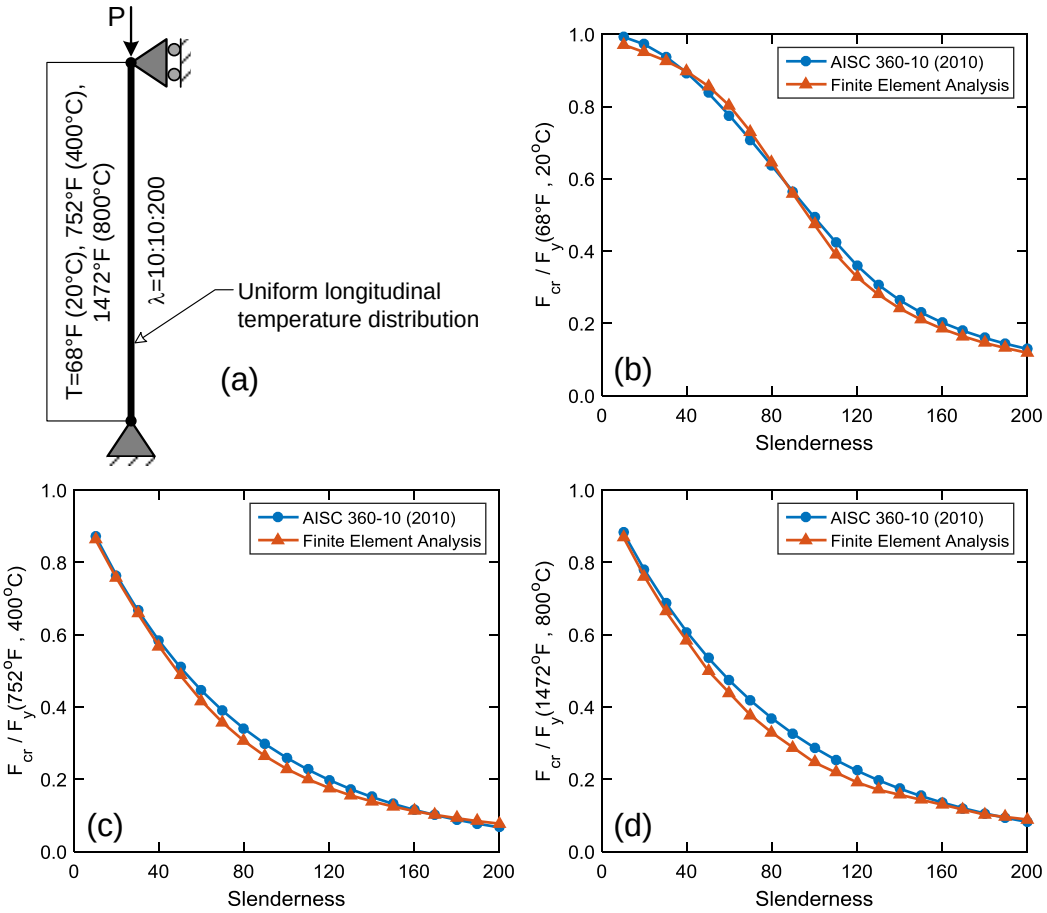

Figure 4: (a) Steel column subjected to a uniform longitudinal temperature and critical buckling stress computed using AISC Specification (AISC 360-10 2010) and finite element analysis at (b) ambient temperature, (c) 752°F (400°C), and (d) 1472°F (800°C)

3. Parametric Study

Four non-uniform longitudinal temperature profiles are chosen for the parametric study to evaluate the effect of the presence or absence of inter-story drift as illustrated in Fig. 5. Fig. 6 shows the critical buckling stress of a pinned-pinned steel column under various levels of inter-story drift ratios and the non-uniform longitudinal temperature profiles discussed previously. As Fig. 6 shows, columns subjected to IDRs have significantly smaller critical buckling stress than those with no IDRs. This indicates that the increase in the inter-story drift causes significant reduction in the critical buckling stress of steel columns. This reduction differs from one temperature profile to another. In conclusion, permanent residual inter-story drift in the steel columns as conclusion of the earthquake can result in significant reduction in buckling capacity of the column.

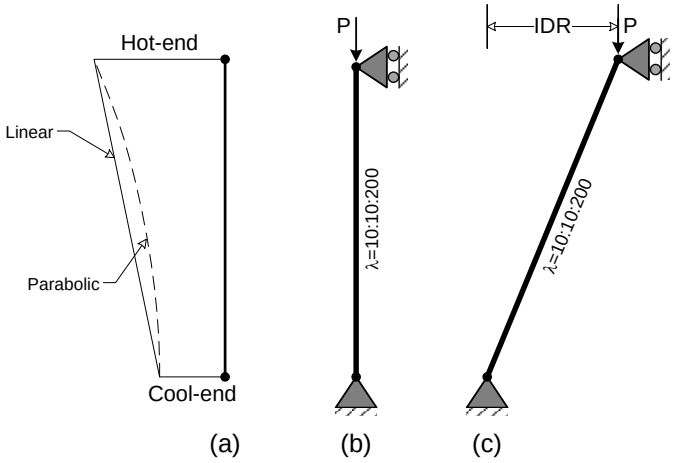

Figure 5: (a) Non-uniform parabolic and linear longitudinal temperature profiles, (b) pinned-pinned column with various slenderness ratios and no IDR, and (c) pinned-pinned columns subjected to IDR

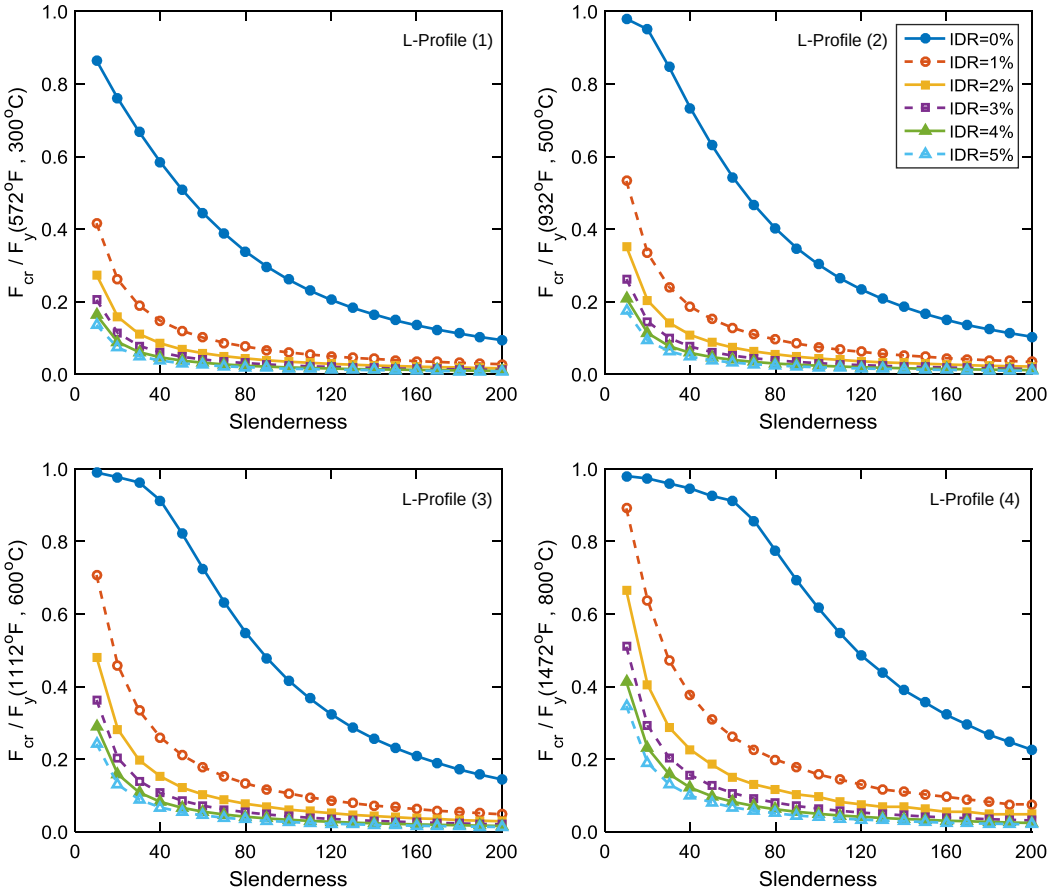

Figure 6: Critical buckling stress in the pinned-pinned steel column at various IDRs and linear non-uniform longitudinal temperature profiles

4. Proposed Design Equations

4.1 Critical Buckling Stress in the Absence of IDR

In this section, equations are proposed to predict the critical buckling stress of steel columns with no IDR subjected to non-uniform longitudinal temperature profiles. The effects of IDR caused by the earthquake demands will be discussed in the next section.

The proposed equation has a similar format to the current equation listed in Appendix 4 of the AISC Specification (AISC 360-10 2010). Two coefficients, p and q, are incorporated in the current design equation per the AISC Specification (AISC 360-10 2010) in order to consider longitudinal variation of mechanical properties of structural steel as per Eq. 7.

$$F_{cr}(T) = \left[(0.42p)^{\sqrt{\left(F_y(T_{max}) / F_e(T) \right)^q}} \right] . F_y(T_{max}) \quad (7)$$

where, $F_e(T)$ is the Euler elastic buckling stress considering non-uniform longitudinal temperature distribution and shall be calculated according to Memari and Mahmoud (2016). Two coefficients, p and q, can be determined according to Tables 2 and 3, and depend on non-uniform longitudinal temperature profiles as listed in Table 1 as well as limit state for the elastic/inelastic buckling of steel columns. It is noted that the term $F_y(T_{max})$ corresponds to the yield stress at the hot-end of the column. The coefficients, p and q, can be also considered as unity for uniform longitudinal temperature profiles to convert Eq. 7 to the current available design equation in Appendix 4 of the AISC Specification (AISC 36-10 2010).

Table 2: The p and q coefficients for $\lambda \le 4.71\sqrt{\frac{E(T_{max})}{F_y(T_{max})}}$

Profile	Longitudinal variation of yield stress (%)	p	q
(1)	0.0	0.90	0.90
(2)	22.0	1.05	1.50
(3)	53.0	1.30	1.80
(4)	89.0	1.30	2.40

Table 3: The p and q coefficients for $\lambda > 4.71\sqrt{\frac{E(T_{max})}{F_y(T_{max})}}$

Profile	Longitudinal variation of yield stress (%)	p	q
(1)	0.0	0.90	0.90
(2)	22.0	0.90	0.90
(3)	53.0	1.18	1.15
(4)	89.0	1.20	1.50

As shown in Fig. 7, the proposed equation is in excellent agreement with the results of the FEA. A relative error of less than 10% is observed in all cases by comparing the predicted critical buckling stresses calculated using the proposed equation and the results of the FEA. The

accuracy of the proposed equation for any non-uniform longitudinal temperature profiles in the absence of IDR was evaluated in Memari and Mahmoud (2016).

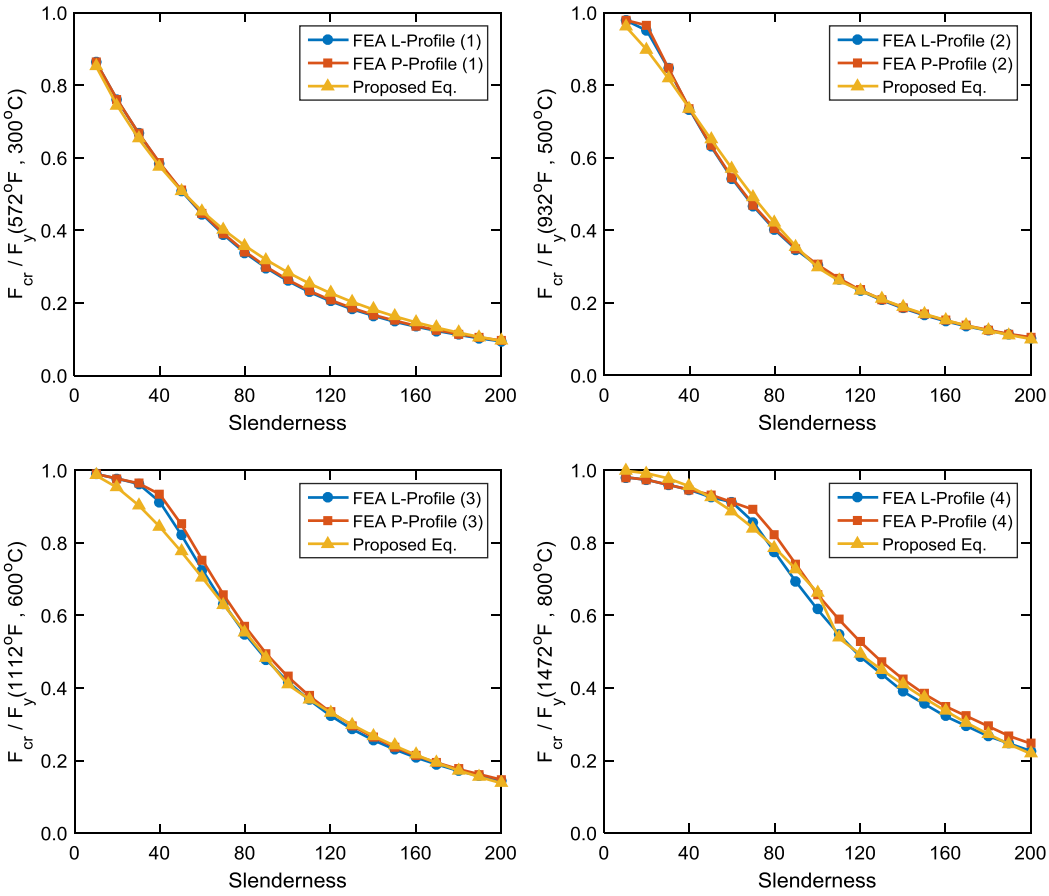

Figure 7: Critical buckling stress computed by FEA and proposed equation in absence of IDR

4.2 Critical Buckling Stress in the Presence of IDR

To consider the effects of permanent lateral deformation in reducing the critical buckling stress of steel columns, a reduction factor, Θ, is introduced as shown in Eq. 8 below:

$$F_{cr}^{idr}(T) = \Theta . F_{cr}(T) \tag{8}$$

where, $F_{cr}^{idr}(T)$ is the critical buckling stress considering the permanent inter-story drift, θ, caused by the earthquake demands. $F_{cr}(T)$ is calculated per Eq. 7. This is also determined in accordance with the desired limit of column slenderness as follow:

For $\lambda \le 4.71\sqrt{\frac{E(T_{max})}{F_y(T_{max})}}$

$$\Theta = (m\theta^{-n}).e^{(r\lambda + s\lambda^2)} \tag{9}$$

where, m, n, r, and s are determined according to Table 4.

Table 4: Coefficients for Eq. 9

Profile	Longitudinal reduction of yield stress (%)	m	n	r	s
(1)	0.00	1.514×10^{-2}	0.8257	-3.237×10^{-2}	2.220×10^{-4}
(2)	22.00	1.686×10^{-2}	0.8280	-3.620×10^{-2}	2.584×10^{-4}
(3)	53.00	2.870×10^{-2}	0.8191	-5.046×10^{-2}	3.682×10^{-4}
(4)	89.00	4.189×10^{-2}	0.8076	-4.777×10^{-2}	2.897×10^{-4}

For $\lambda > 4.71\sqrt{\frac{E(T_{max})}{F_y(T_{max})}}$

$$\Theta = \left(m\theta^{-n}\right).e^{(r\lambda)} \tag{10}$$

where, m, n, and r are determined in accordance with Table 5.

Table 5: Coefficients for Eq. 10

Profile	Longitudinal reduction of yield stress (%)	m	n	r
(1)	0.00	3.871×10^{-3}	0.8211	2.961×10^{-3}
(2)	22.00	3.893×10^{-3}	0.8296	3.374×10^{-3}
(3)	53.00	4.014×10^{-3}	0.8307	3.197×10^{-3}
(4)	89.00	4.075×10^{-3}	0.8371	2.841×10^{-3}

Fig. 8 shows a very good agreement between the proposed equations and the results of the FEA for the critical buckling stress of steel columns under the combined lateral demands and thermal loads. It is observed that the relative error is not constant for various longitudinal temperature profiles and all range of slenderness. In general, there is a relatively larger error for slenderness ratios less than 40 ($\lambda \leq 40$) with a larger error for slenderness ratios between 20-40 in profiles (1) and (2) and a greater error for a slenderness ratio of 10 for profiles (3) and (4). For instance, the proposed equations overestimate the critical buckling stress for a slenderness value of 10 in the profile (4). In conclusion, the proposed equations can predict the critical buckling stress with sufficient accuracy for all range of slenderness. The accuracy of the proposed equations for any non-uniform longitudinal temperature profiles in the presence of IDR was assessed in Memari and Mahmoud (2016).

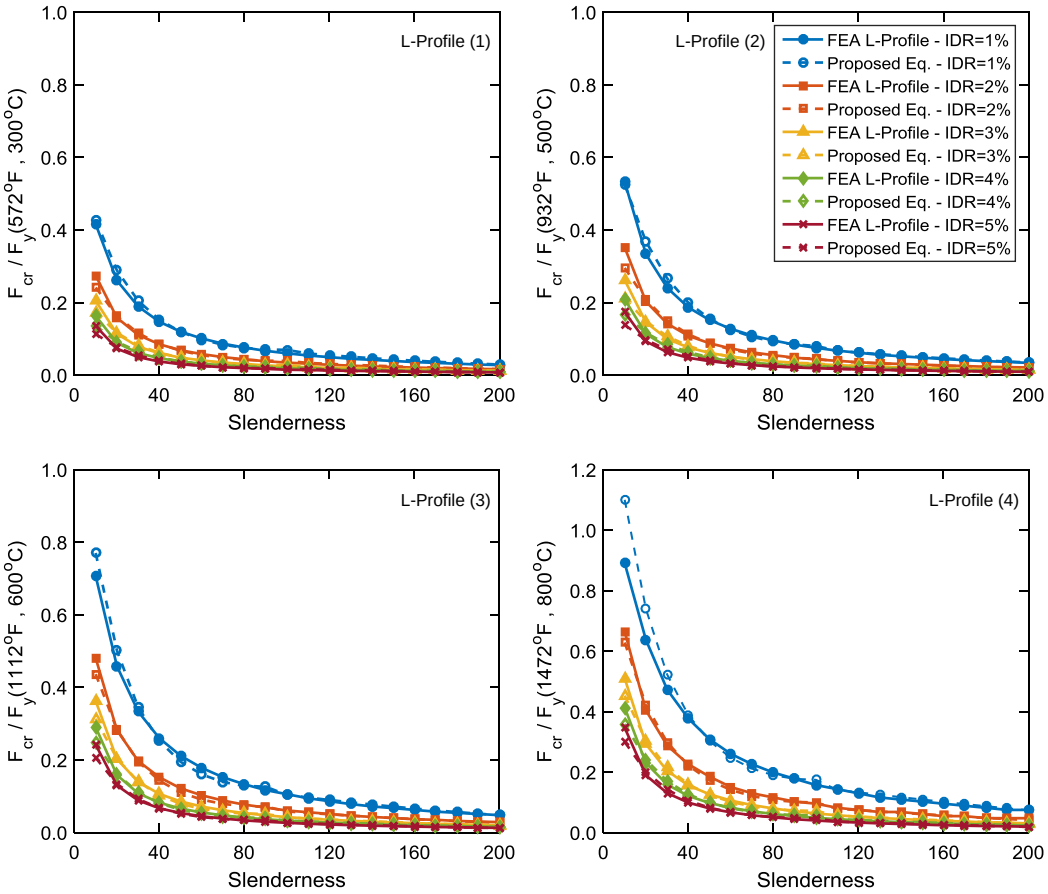

Figure 8: Critical buckling stress computed by FEA and proposed equations in presence of IDR

5. Conclusions

In this paper, a nonlinear finite element approach was introduced for assessing the stability of steel columns under fire loading as well as the earthquake followed by fire loads. This formulation incorporated the effects of residual stresses in W-shape hot-rolled steel sections, temperature-dependent mechanical properties of material, non-uniform temperatures along the length of the column, and initial geometric imperfections. Four various non-uniform longitudinal temperature profiles were considered to allow for assessing the effects of various rates of change in temperature-dependent mechanical properties of structural steel including modulus of elasticity, yield stress, and proportional limit.

Excellent agreement was observed between results of the finite element approach and available strength design equations for steel columns at ambient and uniform longitudinal elevated temperatures. The inclusion of inter-story drift ratio resulted in significant reduction in critical buckling capacity of steel columns with non-uniform longitudinal temperature profiles. A set of design equations was proposed to predict the critical buckling stress of W-shape steel columns for the case of non-uniform longitudinal temperature profiles with and without the presence of inter-story drift. The proposed equations showed a very good agreement with the results of nonlinear finite element analysis (FEA). In the absence of IDR, the comparison between the predicted critical buckling stresses calculated using the proposed equation and the results of the finite element analysis indicated a relative error of less than 10% in all cases. In the presence of

IDR, it seemed that the proposed equations can estimate the critical buckling stress with sufficient accuracy for all range of slenderness.

References

Agarwal, A., Varma, A.H. (2011). "Design of steel columns at elevated temperatures due to fire: effects of rotational restraints." *Engineering Journal*, 4th quarter 297-314.

AISC (2005). "Specifications for structural steel buildings." *ANSI/AISC 360-05*, American Institute of Steel Construction, Chicago, IL.

AISC (2010). "Specifications for structural steel buildings." *ANSI/AISC 360-10*, American Institute of Steel Construction, Chicago, IL.

Carol, I., Murcia, J. (1989). "Nonlinear time-dependent analysis of planar frames using an exact formulation – I. theory." *Computers and Structures*, 33 (1) 79-87.

CEN (2005). "Eurocode 3: Design of steel structures – Part 1-2: General rules – structural fire design." *European Committee for Standardization*.

Franssen, J. M., Talamona, D., Kruppa, J., Cajot, L. G. (1998). "Stability of steel columns in case of fire: experimental evaluation." *Journal of Structural Engineering*, 124 (2) 158-163.

Memari, M. (2016). "Performance of steel structures subjected to fire following earthquake." *Ph.D. Dissertation*, Colorado State University, Fort Collins, CO.

Memari, M., Attarnejad, R. (2010). "An innovative Timoshenko beam element." *Proceedings of 10th International Conference on Computational Structures Technology*, Valencia, Spain.

Memari, M., Mahmoud, H. (2014). "Performance of steel moment resisting frames with RBS connections under fire loading." *Engineering Structures*, 75 126-138.

Memari, M., Mahmoud, H. (2016). "Design formulation for critical buckling stress of steel columns subjected to non-uniform fire loads." *Submitted to AISC Engineering Journal*.

Memari, M., Mahmoud, H., Ellingwood, B. (2014). "Post-earthquake fire performance of moment resisting frames with reduced beam section connections." *Journal of Constructional Steel Research*, 103 215-229.

Memari, M., Mahmoud, H., Ellingwood, B. (2016). "Stability formulation of steel columns subjected to earthquake and fire loads." *Submitted to Journal of Structural Engineering.*

Takagi, J., Deierlein, G.G. (2007). "Strength design criteria for steel members at elevated temperatures." *Journal of Constructional Steel Research*, 63 (8) 1036-1050.